P517410.PDF [Page: 3 of 47]

Copy No. 15

DEFENCE R&D DÉFENSE

A feasibility study of an optical positioning system to correct for dynamic hydrophone array shape variations

Richard D. Dittman

Marentec
6 Jamieson St
Suite 23
Dartmouth, Nova Scotia
Canada B3A 3B7

Contract Number W7707-008102/001/HAL

Defence R&D Canada

Contractor Report

DREA CR 2001-021

March 2001

National Defence Défense nationale

Canada

P517410.PDF [Page: 4 of 47]

Copy No: _____

A feasibility study of an optical positioning system to correct for dynamic hydrophone array shape variations

Richard D. Dittman
Marentec
6 Jamieson St
Suite 23
Dartmouth, Nova Scotia
Canada B3A 3B7

Contract Number: W7707-008102/001/HAL

Defence Research Establishment Atlantic

Contract Report

DREA CR 2001-021

March 2001

517410.PDF [Page: 5 of 47]

104-06252/

Approved by

Francine Desharnais
Scientific Authority

Approved for release by

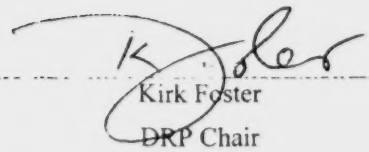

Kirk Foster
DRP Chair

The scientific or technical validity of this Contract Report is entirely the responsibility of the contractor and the contents do not necessarily have the approval or endorsement of Defence R&D Canada

© Her Majesty the Queen as represented by the Minister of National Defence, 2001

© Sa majesté la reine, représentée par le ministre de la Défense nationale, 2001

P517410.PDF [Page: 6 of 47]

Abstract

The following report describes an analysis of a conceptual optical positioning system for measuring the shape of a hydrophone array underwater. The analysis involved the design and construction of a prototype test system comprised of commercially available electronic components. The conceptual system determined the shape of an underwater mooring by positioning tracking targets mounted at fixed points along the mooring. The prototype used a small sensitive black and white camera as the positional detector and high intensity light emitting diodes as tracking targets. The system was examined for its potential range capabilities and spatial resolution underwater. Tests were specifically conducted on the range limits of the system in air, freshwater, and seawater. The results suggested that the spatial resolution of the system was better than 26 cm with target ranges as great as 65 metres. They also indicated, however, that water born attenuators could dramatically reduce the systems operational range limit. Field tests within near-shore waters of Nova Scotia, for example, found range limits closer to 20 metres.

Résumé

Le rapport qui suit décrit une analyse d'un système de positionnement optique conceptuel pour mesurer la forme d'un réseau hydrophone sous-marin. L'analyse portait sur la conception et la construction d'un prototype du système d'essai formé de composantes électroniques disponibles au niveau commercial. Le système conceptuel a déterminé la forme d'un corps mort sous-marin par le positionnement de cibles de poursuite montées sur des points fixes le long du corps mort. Le prototype a utilisé une petite caméra sensible en noir et blanc comme détecteur de positionnement et des diodes émettrices de lumière à haute intensité comme cibles de poursuite. On a étudié les capacités potentielles à distance et le pouvoir séparateur spatial sous l'eau du système. On a mené des essais précis sur les limites du système relativement à la distance dans l'air, dans l'eau douce et dans l'eau de mer. Les résultats supposent que le pouvoir séparateur spatial du système était supérieur à 26 cm lorsque les cibles étaient situées aussi loin que 65 mètres. Toutefois, ils ont également révélé que les atténuateurs formés par l'eau pourraient grandement réduire la portée opérationnelle du système. Des essais sur le terrain effectués dans les eaux à proximité du rivage en Nouvelle-Écosse, par exemple, ont révélé que la portée se situait plus près de 20 mètres.

This page is left blank

This page is left blank

P517410.PDF [Page: 8 of 47]

Executive summary

Oceanographic measurements made with mooring technologies are often plagued by the action of ocean currents upon the cables or ropes used to secure instruments at depth. These cables, ropes, or harness assemblies drift, and/or, strum in response to the friction and velocity of water flowing by them. For underwater acoustics work, knowing the precise position of individual hydrophone along an array is often critical.

Several solutions exist to estimate the position of moorings as a function of time, the traditional one using depth and tilt sensors clipped along the array. These solutions, however, are often expensive, power consuming, or otherwise inadequate to fully describe the 3-D shape and motion of the array.

It has only been in the past decade that low-cost surface-mount digital processing systems and associated electronics have become economical. This availability has lead to the development of simplified, smaller, and more powerful sampling and processing electronics, some of which could serve together to create a low-cost, low-power, positioning system. The conceptual system determined the shape of an underwater mooring by positioning tracking targets mounted at fixed points along the mooring. The prototype used a small sensitive black and white camera as the positional detector and high intensity light emitting diodes as tracking targets. The system was examined for its potential range capabilities and spatial resolution underwater.

The results suggested that the spatial resolution of the system was better than 26 cm with target ranges as great as 65 metres. They also indicated, however, that water born attenuators could dramatically reduce the systems operational range limit. Field tests within near-shore waters of Nova Scotia, for example, found range limits closer to 20 metres.

Dittman, R., 2001. A Feasibility Study of an Optical Positioning System to Correct for Dynamic Hydrophone Array Shape Variations. DREA CR 2001-021 Defence Research Establishment Atlantic.

17410.PDF [Page: 9 of 47]

Sommaire

Les mesures océanographiques effectuées à l'aide des technologies des corps morts sont souvent modifiées par l'action des courants océaniques sur les câbles ou les cordes utilisées pour garder les instruments en profondeur. Ces câbles, cordes ou harnais dérivent ou se déplacent en raison du frottement et de la vitesse de l'eau. Pour les travaux d'acoustique sous-marine, il est souvent nécessaire de connaître la position précise des hydrophones individuels situés le long d'un réseau.

Il existe plusieurs solutions pour évaluer la position des corps-morts comme une fonction du temps, la plus connue consistant à utiliser des capteurs d'inclinaison et de profondeur alignés le long du réseau. Ces solutions sont toutefois souvent coûteuses, elles consomment de l'énergie ou sont autrement inadéquates pour décrire pleinement la forme 3-D et le mouvement du réseau.

C'est seulement au cours de la dernière décennie qu'il est devenu économique d'utiliser les systèmes de traitement numérique peu coûteux montés en surface et l'équipement électronique connexe. Cette disponibilité a entraîné la mise au point d'équipement électronique de traitement et d'échantillonnage plus petit, plus puissant et plus simple à utiliser, dont certains pourraient servir à créer des systèmes de positionnement peu coûteux et consommant peu d'énergie. Le système conceptuel a déterminé la forme d'un corps-mort sous-marin par le positionnement des cibles de poursuite montées sur des points fixes le long du corps-mort. Le prototype a utilisé une petite caméra sensible en noir et blanc comme détecteur de position et des diodes émettrices de lumière à haute intensité comme cibles de poursuite. On a étudié les capacités potentielles à distance et le pouvoir séparateur spatial sous l'eau du système.

Les résultats suggèrent que le pouvoir séparateur spatial du système était supérieur à 26 cm lorsque les cibles étaient situées aussi loin que 65 mètres. Toutefois, ils ont également révélé que les atténuateurs formés par l'eau pourraient grandement réduire la portée opérationnelle du système. Des essais sur le terrain effectués dans les eaux à proximité du rivage en Nouvelle-Écosse, par exemple, ont révélé que la portée se situait plus près de 20 mètres.

Le système démontre un fort potentiel lorsqu'il est utilisé dans les petits systèmes acoustiques de faible énergie comme les systèmes à déploiement rapide.

Dittman, R., 2001. A Feasibility Study of an Optical Positioning System to Correct for Dynamic Hydrophone Array Shape Variations. DREA CR 2001-021 Defence Research Establishment Atlantic.

P517410.PDF [Page: 10 of 47]

Table of contents

Abstract i

Executive summary iii

Sommaire iv

Table of contents v

Introduction 1

The Conceptual Model 2

An Analysis of Light Propagation Underwater 10

The Prototype 15

Selection of an Appropriate Camera 15

Dynamic Range and Signal Processing with the Cameras Automatic Gain Control 16

Range Limit Testing of the System 17

Spatial Resolutions Limitations of the Camera 17

The Underwater Camera Package 18

LED Projector Targets 20

LED Projector Design I 21

LED Projector Design II 22

Projector Beam Patterns 24

Field Testing the Prototype System 25

Results and Discussion 27

Range Limit Testing in Air 27

Range Limit Testing in Water 28

How the Camera Viewed the Targets 29

Conclusions 34

References 34

Introduction

Oceanographic measurements made with mooring technologies are often plagued by the action of ocean currents upon the cables or ropes used to secure instruments at depth. These cables, ropes, or harness assemblies drift, and/or, strum in response to water flowing by them. The traditional approach to solving this problem has been to maintain a high degree of tension on the mooring cables or ropes by coupling a large anchor to a large buoy. This approach, unfortunately, requires the use of a large support vessel and with today's support budgets growing increasingly smaller, its practicality has been decreasing proportionately. To overcome this dilemma, instrumentation developers have provided a number of solutions to oceanographers. The most significant of these solutions is the manufacturing of small low cost pressure sensors, which can provide the depth variations associated with the motion of the moorings in the currents. Others include solid state gyro systems, acoustic positioning transducers or tilt sensors. For most oceanographic applications, the depth sensor is sufficient to compensate for motion in the moorings, but for naval acoustic moorings, depth corrections alone are not enough.

Since the measurement of the sound propagation vectors is obtained from the serial excitation of hydrophones along a linear or pre-defined spatial vector, hydrophone arrays are extremely sensitive to the effects of strumming and angular deflections caused by the action of currents. Deviations from the assumed orientation and location of hydrophones in the array introduce error directly into the estimation of the propagation vectors and can even inhibit the excitation of certain hydrophones. Strumming at certain frequencies can also actually introduce artificial acoustic noise to the background received by the hydrophones. Only a time series analysis of the actual 3-D positioning of an array's hydrophones can accurately quantify these errors in the measured sound propagation vector. Unfortunately, such positioning information has in the past, been difficult to obtain without the aid of complex and expensive positioning systems. It has only been in the past decade that low-cost surface-mount digital processing systems and associated electronics have become economical. This availability has lead to the development of simplified, smaller, and more powerful sampling and

P517410.PDF [Page: 12 of 47]

processing electronics, some of which could serve together to create a low-cost positioning system. One area of electronics of particular interest in this application is the area of opto-electronics. This technology has been developing especially fast in response to its role in fibre optic communications and imaging applications. Advances include the development of low power, high intensity light emitting diodes (LEDs) and numerous different, compact, low power, high resolution video cameras. The following report will examine the feasibility of using these off-the-shelf technologies in a hydrophone positioning system.

The Conceptual Positioning System

The conceptualized system proposed in this report incorporates high intensity LEDs as tracking targets viewed by a sensitive black and white camera. The x-y coordinates of the targets map the shape of the array when coupled with a z coordinate from the pressure transducers at each target.

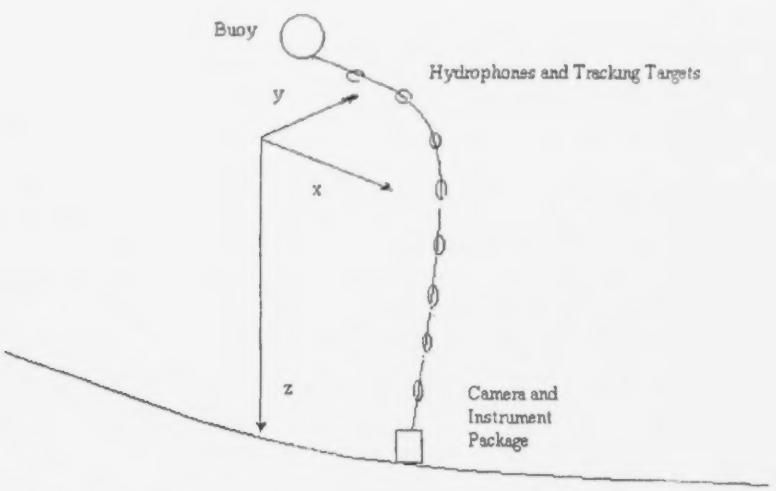

Figure 1: A diagrammatical representation of how the conceptual positioning system might be deployed at sea In the diagram a series of targets are viewed from below by the camera and their positions mapped relative to the camera's orientation.

P517410.PDF [Page: 13 of 47]

The drawing in Figure 1 shows the system with the camera mounted on the sea bottom and a linear array deployed above. In this particular image all target light sources are shown illuminated. In the final system design however, the targets will be turned on sequentially, to sort their order in the image. This procedure is expected to prevent the situation shown in Figure 2 and should identify potential cross over in the array. It should also allow the camera to adjust its video gain to suit each individual target in its field of view. The result should provide a video signal more like the one shown in Figure 3 .

Figure 2: A diagrammatical representation of how the targets on the array in Figure 1 might look if viewed on a television screen. Each splotch in the image portrays the image of a single target. The images will decrease in size and intensity as z or their axial range increases.

where only the peak of a single target can be seen in any one video frame. The maximum of this peak provides a useful triggering point with which to reference the target's position within the video frame and the negative going synchronization pulses which delineate it, in time.

?517410.PDF [Page: 14 of 47]

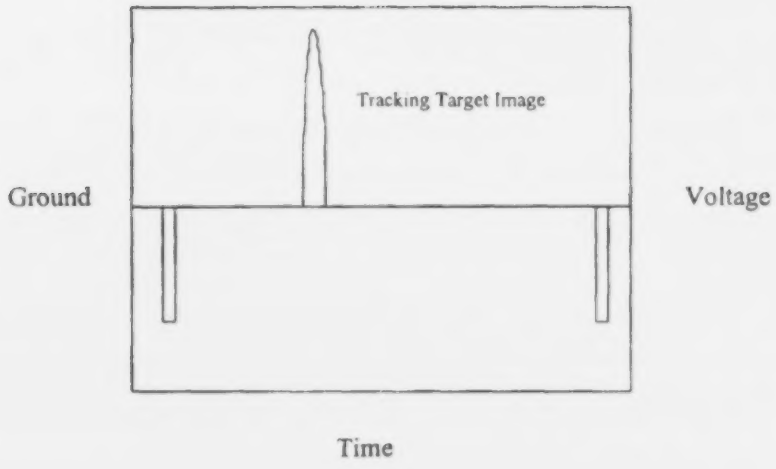

Figure 3: A diagrammatical representation of an oscilloscope sweep of the video signal derived from the image of a tracking target in the dark. The time between the negative going, square frame synchronization pulses is 16 ms. The amplitude of the positive going image peak is 1 V.

The actual x and y coordinates are calculated from the time offset of the target image and the frame and line sync. pulses. The frame sync. pulses are used to reference the y coordinates and repeat at 16 ms intervals. The line sync. pulses in contrast reference the x coordinate and repeat every 50 μs inside each frame (See Figures 4 and 5). The time offset of the target's signal is actually directly related to the angular displacement of the peak off of the center of the lens, since the image is spherical. Offsets therefore, must first be converted into angles θ', ϕ' describing their coordinates in an x-y frame of reference. With these and an estimate of z, they can be mapped within an x, y, and z reference grid as in Figure 6.

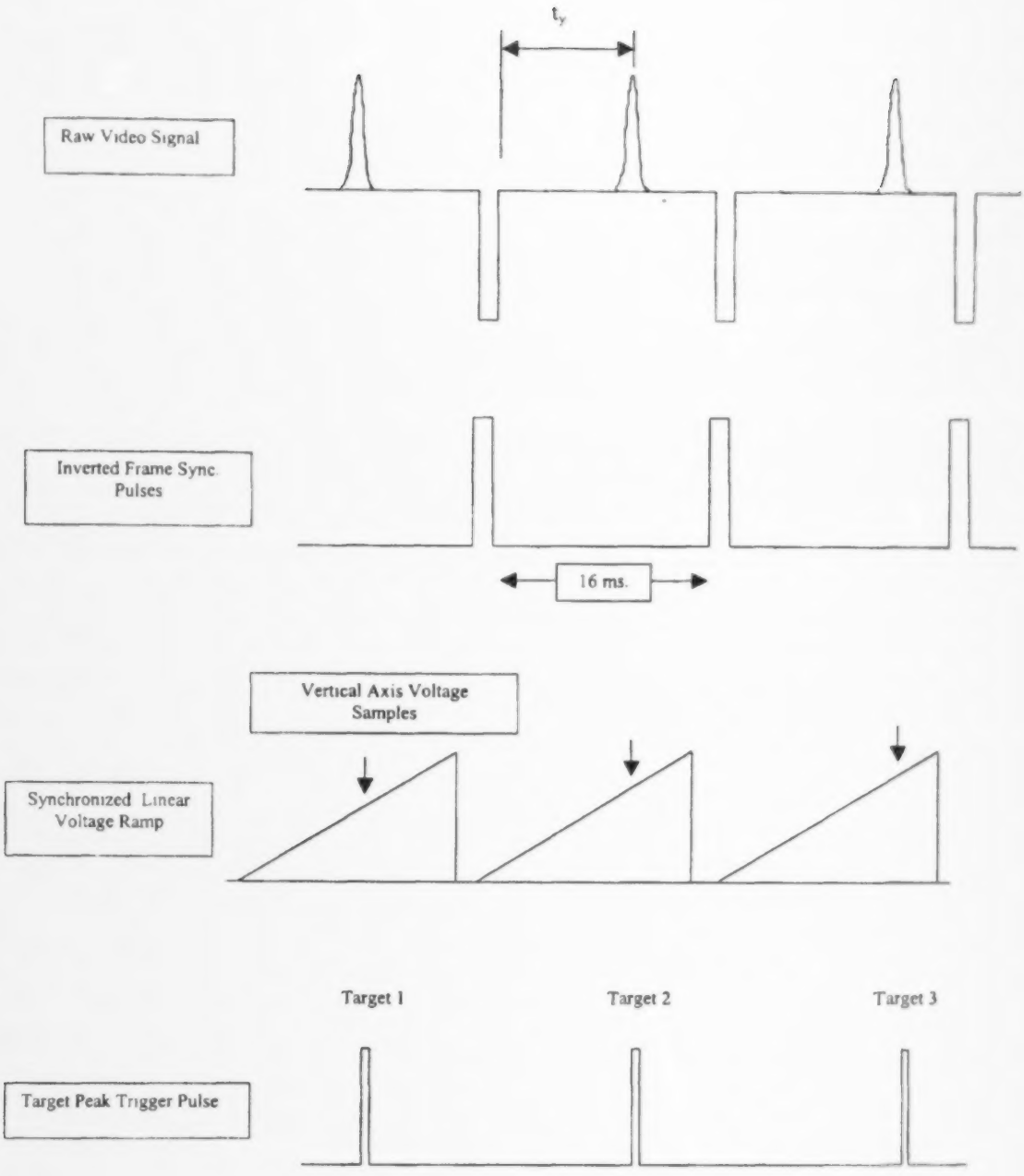

Figure 4: A timing diagram of the processing of the raw video signal to extract the vertical or y axis information of the tracking target's image as seen by the bottom deployed camera. The timing diagrams are simplified and do show the line sync. pulses which are normally also present between the frame sync. pulses.

P517410.PDF [Page: 16 of 47]

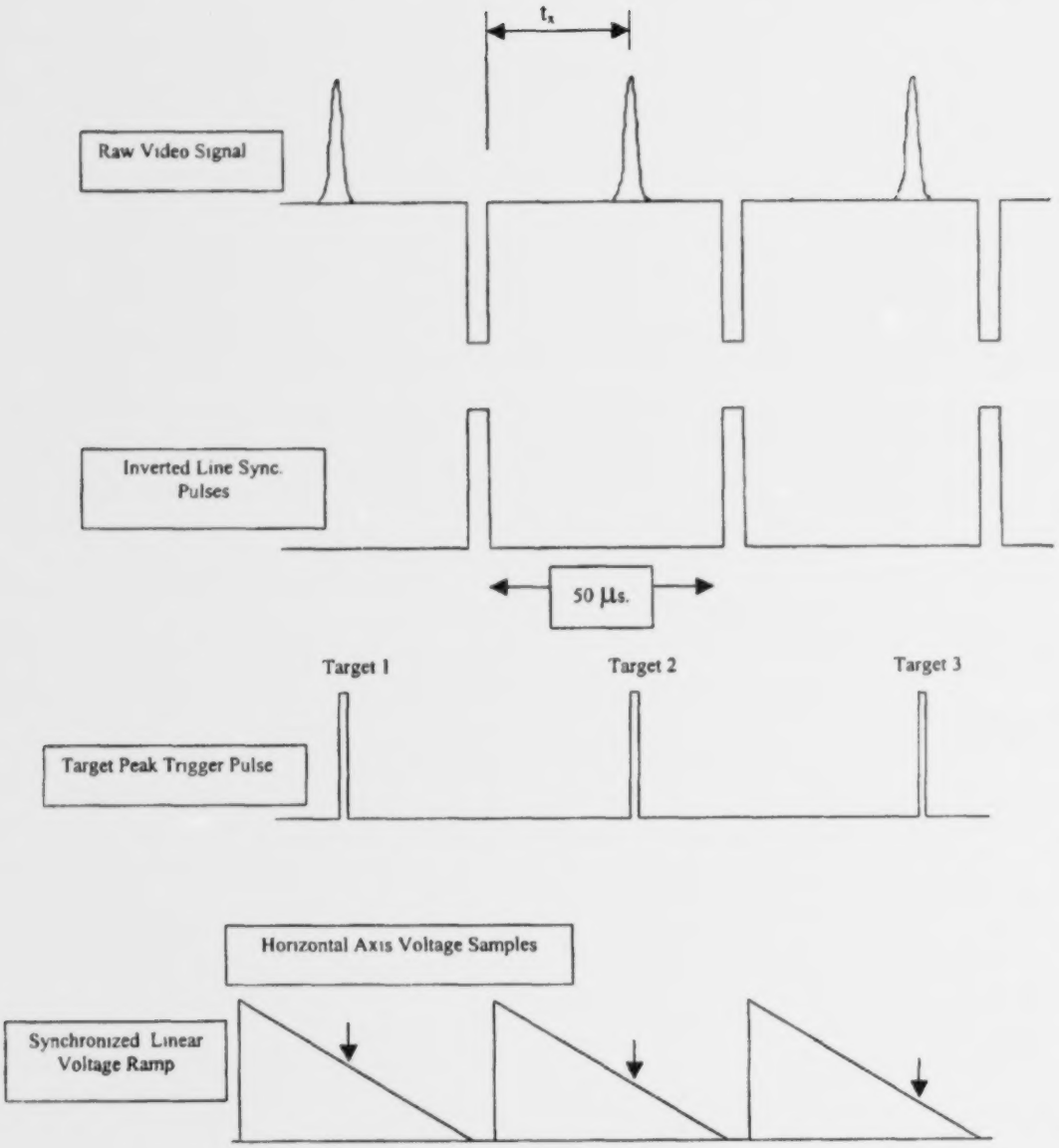

Figure 5: A timing diagram of the processing of the raw video signal to extract the horizontal or x axis information of the tracking target images as seen by the bottom deployed camera. The timing diagrams are simplified and do not show the frame sync. pulses. Typically there will be as many as 400 line pulses within a given frame period.

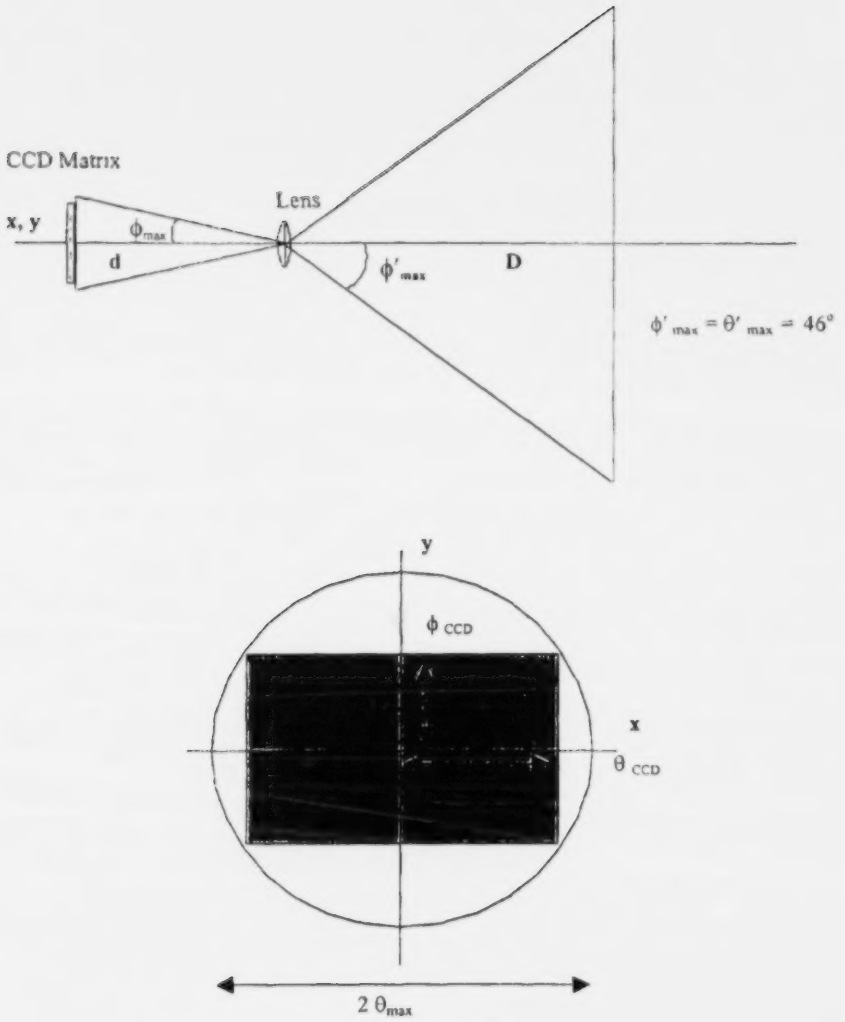

Figure 6: The top diagram presents a side view of how the x, and y coordinates of a target image are derived from the position of the image upon the CCD matrix of the camera. The lower diagram shows the circle defining the limit of images created with the camera lens. The diagram also shows a representation of the CCD matrix within the image limits.

For the **X axis**:

(1) $$\theta' = \mathbf{F_{lens}}\,(2\,t_x / T_{line} - 1)\;\theta_{CCD}$$

where t_x = Time offset of the peak relative to the line sync. pulse

T_{line} = Period of the line sync. pulse.

$\mathbf{F_{lens}}$ = The lens compression factor (i.e. $\theta' = F_{lens}\,\theta$)

and θ_{CCD} = Half the angular field of view along the x axis of the CCD matrix.

For the **Y axis**:

(2) $$\phi' = \mathbf{F_{lens}}\,(2\,t_y / T_{frame} - 1)\;\phi_{CCD}$$

where t_y = Time offset of the peak relative to the frame sync pulse.

T_{frame} = Period of the frame sync. pulse.

and ϕ_{CCD} = Half the angular field of view along the y axis of the CCD matrix.

x and y coordinates can then be calculated as follows:

(3) $$\mathbf{X = D \tan \theta' \quad and \quad Y = D \tan \phi'}$$

where D is the range along the Z axis and is measured by the depth difference between the target and the camera.

The values of t_y and t_x can be measured and displayed in a number of different ways, but two seem most suitable. The first requires the use of a timing circuit triggered on and off

with the sync. pulses and the image peak or the output of a high speed comparator sampling it. The only complication with this approach is the number of separate counters required to give the circuit a resolution with the camera resolution or better. A single 8-bit counter for example, would not be sufficient. Only a 10-bit counter or three decade counters would suffice. The alternative approach uses a 10-bit analog to digital converter to translate t_y and t_x into digitized voltages with the timing schematics described in Figures 4 and 5. In the schematics, synchronized linear voltage ramps are digitized with fast, 10-bit analog to digital converter chips. The 10-bit signals are then stored in respective latches for downloading at the end of each video frame. The entire circuit would require only a 555 timer and a slow signal diode to provide the two different linear voltage ramps, a 40 MHz TTL clock, two 10-bit or greater latches, two high speed comparators or high speed logic switches, and two 20 MHz or faster, 10-bit analog to digital converter. The resulting circuit would resemble that presented in Figure 7.

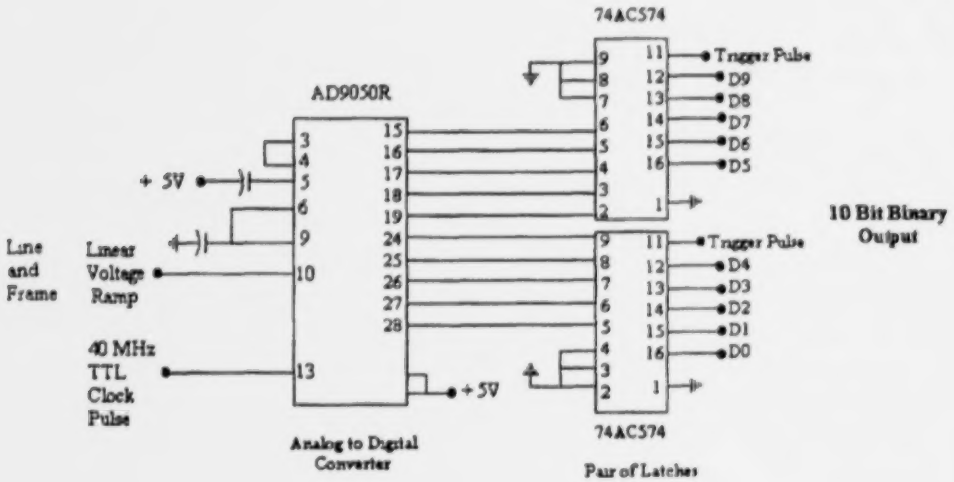

Figure 7: A schematic of the circuit to convert the t_x and t_y into a digital format. The diagram describes both the frame and line sampling circuits since only the linear voltage ramp inputs differ between the circuits. Both use the one trigger signal generated from the comparison of the image peak in the raw video signal with a reference voltage as in Figures 4 and 5.

An Analysis of Light Propagation Underwater:

The largest hindrance to the operation of the conceptual system is believed to the limitation imposed by the attenuation of the tracking target's light by the seawater. Attenuation by absorption and scattering in water is generally, several orders of magnitude greater than that in air. It can therefore, severely limit the operational range of the system in the field. To date however, no operational envelope has been published for an optical positioning system.

In a simplified model of the propagation of light from the target to the camera, the amount of the light received by the camera can be described using the light ray geometry presented in Figure 8. Here a conical beam of light is emitted by the projector towards a camera with a circular aperture at some range D. The camera in this particular instance is assumed to be aligned with the axis of the tracking target's beam cone.

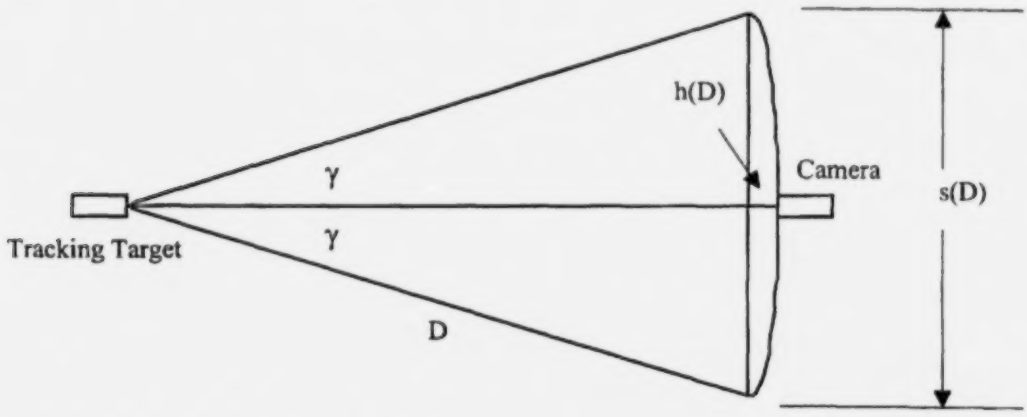

Figure 8: A diagrammatical representation of a side view of the light beam produced by a tracking target. Here the beam is projected towards the camera at some distance D. s(D) represents the chord subtending the emission sphere at a distance D from the projector.

In the model, light is lost from the camera's view through two different processes. The first is by the inherent dispersion of the light source. This term can be described through the ratio of the camera's aperture area A_{camera} to the cross sectional area of the beam A_{beam} as follows, if we assume that scattering only results in a loss of light and multiple scattering does not occur:

(4) $$E = E_o \; \Gamma(D) \; \varphi(\lambda) \; A_{camera} \; / \; A_{beam}(D)$$

(5) $$E = E_o \; \Gamma(D) \; \varphi(\lambda) \; \pi \; r_a^2 / \; K(\gamma) \pi \; D^2$$

where r_a is the camera aperture radius, E is the photon flux per unit area, E_o is the photon flux at the emitter, $\varphi(\lambda)$ is wavelength dependant sensitivity of the camera, D is the range to the camera, and $K(\gamma)$ is the angular constant describing the dispersion of the beam. $\Gamma(D)$ describes the range dependant pixel normalizing factor and in its simplest form can be determined by the ratio of the CCD matrix's element area to the area of the target image on the CCD surface. This term increases with D and with a wide angle camera lens, quickly approaches unity where the entire image resides on a single element in the CCD matrix. Within the context of the conceptual system only the center of the target image where intensities are greatest is of interest. This portion of the beam may only contribute a small fraction to the total value of E seen by the camera. Values as small as 0.01 for $\Gamma(D)$ at close ranges (i.e. < 5 m) would not be unusual.

E therefore, can be expanded as follows, using the diagram in Figure 9 as a reference:

(6) $$A_{beam}(D) = \pi \; (s(D)^2 + h(D)^2) / 4$$

where,

(7) $$s(D) = 2 \; D \sin \gamma \qquad h(D) = D \; (1 - \cos \; \gamma)$$

and,

(8) $$K(\gamma) = \sin^2 \gamma + \pi \cos^2 \gamma - 2 \pi \cos \; \gamma + \pi$$

P517410.PDF [Page: 22 of 47]

$$(9) \qquad E = E_o \ \Gamma(D) \varphi(\lambda) \ r_a^2 / ((\sin^2 \gamma + \pi \cos^2 \gamma - 2\pi \cos \gamma + \pi) D^2)$$

γ is the dispersion angle of the projector beam, s(D) is cord subtending the dispersion sphere and is calculated from the range D and γ. The result suggests that the amount of light seen by the camera will decrease proportional to the inverse square of the range to the target. The rate of this decrease however, will be scaled by the camera sensitivity, the area of the camera aperture, and $K(\gamma)$.

The second loss results directly from the attenuation of light by the water and materials in it. The process is random and therefore, can be described through a Beer-Lambert type probability relation as follows in Equation 10:

$$(10) \qquad P(0) = e^{-\alpha D}$$

where α is the attenuation cross-section or coefficient for the projector's light passing through a water column of length D. The relation essentially predicts the probability P(0) that a photon will not be scattered or absorbed out of the view of the camera. Since this probability is independent of the beam dispersion it can be used to compound the dispersion loss as follows:

$$(11) \qquad E = E_o \ \Gamma(D) \varphi(\lambda) \ (r_a^2 / K(\gamma) D^2) \ e^{-\alpha D}$$

The final relation therefore, shows that while the beams light flux decreases as the square of the range, it simultaneously decreases exponentially as a result of attenuation. The dispersion part of the relation can be controlled optically, but attenuation is dictated entirely by the properties of the water column. The optimum tracking target then, should be a light projector with a narrow beam of light to minimize $K(\gamma)$ and losses due to beam dispersion. The beam however, cannot be so narrow that it cannot be seen by the

camera when the tracking target is tilted by a curvature in the mooring. The light source used in the target should also have as much of its emission energy within the transmission window of seawater as possible. This will minimize the losses in E due to the absorption by water. Figure 9 for example shows how different LED (Light Emitting Diodes) could be useful as light sources in the tracking targets.

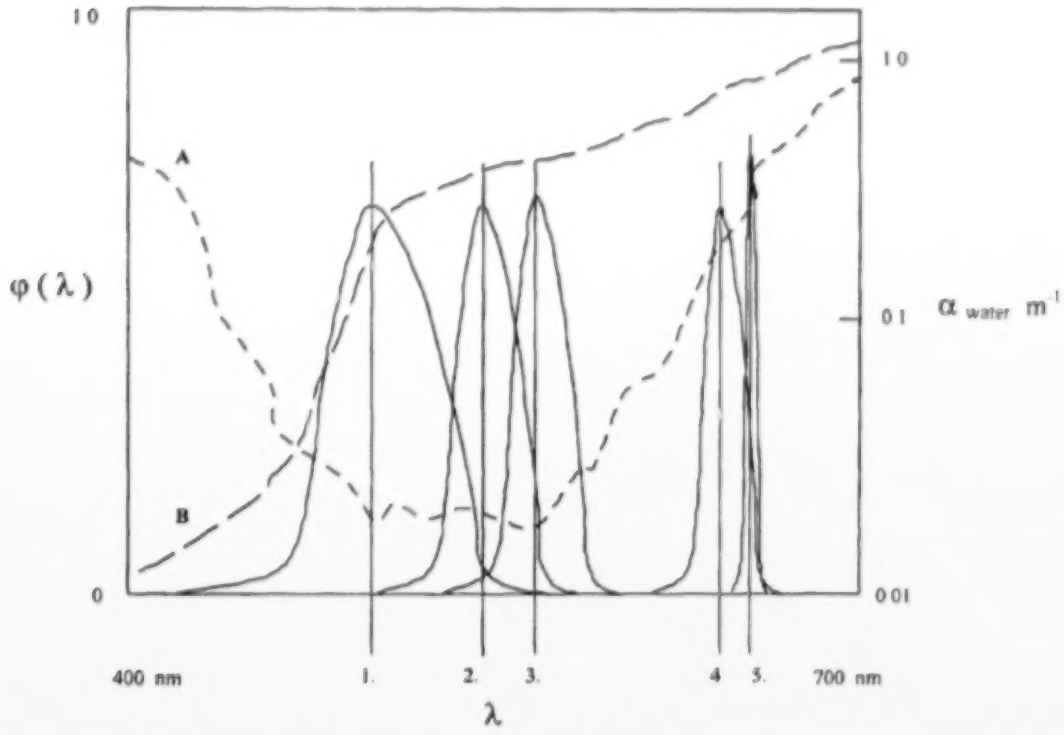

Figure 9: The following is a diagram showing the emission peaks of a number of different semiconductor light sources relative to the attenuation spectrum of pure water **A**, and the sensitivity curve **B** of silicon base detectors. The attenuation curve is based on that presented for water by Morel (1974) and the sensitivity curve was based upon that presented in the TRW Optoelectronics Data Book (1985). Peak 1. represents the normalized emission peak of a silicon carbide semiconductor and has a peak centered at 430 nm. Peak 2. is that of the sodium nitride semiconductor and is centered at 470 nm. Peak 3. is generated by a new sodium nitride hydbrid semiconductor and is centered at 490 nm. Peaks 4. and 5. are generated by hybrids of the gallium arsenide semiconductors and are centered near 640 and 660 nm respectively. Peak 5. actually represents the emission of a semiconductor laser and is extremely monochromatic as a result.

P517410.PDF [Page: 24 of 47]

The spectra in Figure 9 suggest that the sodium nitride semiconductors are the most suitable light sources for the tracking targets. They can be readily detected by a silicon based detector and, they emit within the transmission window of water. The only factor working against their use results from natural competition with phytoplankton. Phytoplankton have evolved to efficiently utilize light within the water transmission window part of the visible spectrum and can be extremely effective in attenuating the light of the tracking targets. Fortunately, their attenuation coefficient is proportional to the concentration of the organisms and most of them are restricted to the water column above the thermocline. Regardless, α should actually be written as $\alpha(\lambda,c(D))$ where:

$$\alpha(\lambda, c(D)) = \alpha_{water}(\lambda) + \alpha_{algae}(\lambda, c(D)) \quad (12)$$

and,

$$\alpha_{algae}(\lambda, c(D)) = \varepsilon_{absorpt.}(\lambda, c(D)) + \varepsilon_{scatter}(\lambda, c(D)) \quad (13)$$

$\alpha_{water}(\lambda)$ is the wavelength (λ) dependant attenuation due to water. $\alpha_{algae}(\lambda,c(D))$ is the wavelength, and cell concentration (c(D)) dependant attenuation coefficient comprised of an absorption component $\varepsilon_{absorption}(\lambda,c(D))$ and a scattering component $\varepsilon_{scatter}(\lambda,c(D))$. Generally, $\alpha_{algae}(\lambda,c(D))$ increases exponentially between the surface and the thermocline (Lewis et al. ,1983). It then drops to near zero at the bottom of the thermocline and remains near zero with increased depth. For depths above the thermocline α becomes:

$$\alpha(\lambda, c(D)) = \alpha_{water}(\lambda) + \int_0^D \alpha_{algae}(\lambda, c(D))\, d(D) \quad (14)$$

Below the thermocline, α can be approximated by α_{water} (See Figure 9), though additional depth dependant attenuators may be present. These can include refractive

index microstructure from thermal and haline mixing near the pycnocline, and scattering by suspended particles such as marine snow.

The Prototype

To gain an appreciation of the conceptual system's limitations, a simplified model or prototype was designed and built with off the shelf technologies. The prototype system employed a sensitive black and white video camera as a spatial detector, and a customized LED projector as a target. With it, the parameters most affecting the functioning of the conceptual system were examined both in the lab and in the field. These parameters included the camera's sensitivity, dynamic range, and spatial resolution. It also included the properties of the tracking targets and the factors affecting the propagation of their light in the water.

The prototype system used for testing in this report only provided a positional information through the raw video output of the camera. A conceptualized design of the appropriate circuitry needed to convert the raw video signal into actual spatial coordinates however, was used to examine what features would be required for the optimal functioning of the entire system.

Selection of an Appropriate Camera:

The selection of the best black and white camera was crucial to the proper functioning of the positioning system. This selection process had to examine both the technological and cost aspects of the camera since cost was expected to be a major limitation in the final design of the system. Fortunately, society's need for security monitoring systems has helped by stimulating the camera market to design and manufacture a large variety of low cost, high sensitivity, compact, black and white cameras. These cameras are now available in a number of different packages, and sensitivities to low light levels. Typically, the board cameras are the least expensive and are sensitive down to light levels near 0.4 Lux. Some of the higher end cameras however,

P517410.PDF [Page: 26 of 47]

are as much as an order of magnitude more sensitive and yet, are still reasonably priced. One such camera was the C.V. 5005-B manufactured by Channel Vision in Costa Mesa, California. This camera called a bullet camera as a result of its small cylindrical shape, was packaged within a metal cylinder, just under 2 cm. in diameter and 5 cm. in length and had a full field of view of 92°. The C.V. 5005-B is quoted as being capable of resolving images at illuminations as low as 0.05 Lux. It has a large CCD matrix which provides it with a video resolution of 420 lines, 40 lines more than most less expensive cameras. Only one other more expensive camera, a Watec Black and White ½" video camera had comparable or better specifications. The C.V. 5005-B retailed for about $200 Canadian and are readily available on the market.

Dynamic Range and Signal Processing with the Camera's Automatic Gain Control:

While low light sensitivity was a crucial in the design of the camera selected, dynamic range was felt to be equally if not more important. One of the key features of the proposed prototype positioning system was the use of a camera with Automatic Gain Control or an AGC amplifier since the targets would appear with widely varying intensities. Their video signal however, would still have to be used to trigger a voltage comparator and/or an analog to digital converter chip to derive positional information. The AGC amplifier is designed to compensate for intensity variations automatically by adjusting its gain until the brightest pixel in the signal has a voltage of approximately 1V. This means that as long as the intensity of an LED projector is within the amplification limits of the camera and, it is the brightest object in the camera's field of view, its image will have an amplitude of 1 V in the video signal. This constant amplitude peak is extremely useful and, even imperative for triggering a timing circuit. The most efficient camera for positioning therefore, must have an AGC amplifier with an extremely wide swing in gain to optimize on the detection of targets both near and far. The C.V. 5005-B appeared to posses such an amplifier and could view both extremely intense and weak light sources with equal clarity.

P517410.PDF [Page: 27 of 47]

Range Limit Testing of the System:

To get a good appreciation of how well the camera could resolve a target at the low light extremes of the operational envelope, a series of simple range tests were conducted on land. In these tests a C.V. 5005-B camera was mounted at a fixed distance from a single blue LED target and its video signal was monitored with a television and a 20 MHz oscilloscope. The intensity of the LED target was then varied by adjusting its forward current to see at what point it could no longer trigger a comparator comparing a video signal with a user controlled voltage threshold. This approach was effective in showing that LEDs could be seen by the camera in air but quantitative comparisons to similar attenuations scenarios underwater were impossible. This was because no information on the LED's intensity versus forward current relationship was available. Another more quantitative approach using calibrated neutral density filters was adopted. With this approach, two polarized filters, each with a 13% transmission were stacked upon one another in front of the camera to simulate a water column with a total transmission of 1.69% or a value of 0.0169 for P(0) from Equation 10. The range (D) to the target was then varied and the video signal was monitored as before, to see when the target could no longer be detected. This provided threshold testing with both a simulated variation in the attenuation coefficient and a real variation in the dispersion component of Equation 11. Ranges between 3 and 65 metres for example, equated to simulated water α s between 1 4 and 0.06 m^{-1}. These values were felt to be representative of coastal marine waters but, were large in comparison to the 0.03 m^{-1} estimated for filtered seawater (Tyler and Smith, 1970 ; Jerlov and Nielsen, 1974) .

Spatial Resolution Limitations of the Camera:

While the sensitivity and the dynamic gain determined the operational envelope of the camera, the physical size and the number of elements its CCD matrix determined its ability to resolve spatial information within this envelope. The C.V. 5005- B bullet camera uses a 512x496 matrix of light sensitive elements which are 9.6 x 7.5 μm in size. These particular elements are large relative to those of color cameras and, are therefore,

PS17410.PDF [Page: 28 of 47]

more sensitive to low light levels. The full size of the entire matrix is 8.5 mm^2 and this is illuminated through a 3.6 mm lens with a full field of view of 92°. Physically this means that the C.V 5005-B camera can resolve angular displacements on the order of 0.185°. The spatial resolution associated with this will vary linearly with the axial range (D) within the viewing cone of the camera but will be approximately 10 cm/pixel at a range of 33 metres. Unfortunately, the video signal generated by the CCD amplifier board is only capable of providing a 420 line output. This means that 420 horizontal sweeps are generated per image frame. Single pixels however, should remain resolvable within each of the lines. Cameras with larger CCD matrices could be used to improve this resolution but their outputs would still be limited by television signal standards. If greater resolutions are truly needed, the simplest solution is to use a convex lens in line with the existing camera lens. The lens would increase the image size at the CCD matrix and only at the expense of the field of view. At worst however, resolutions will always be better than 26 cm/pixel since beam attenuations are expected to restrict operational ranges to within 65 metres.

The Underwater Camera Package:

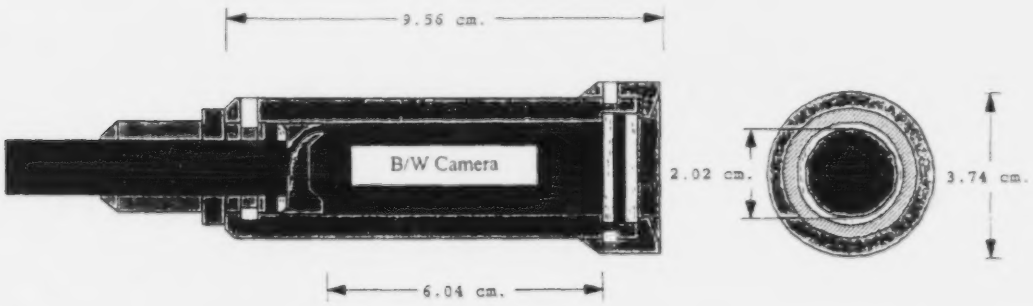

Figure 10: A coss-sectional and end on view of the underwater video camera housing

In order to test the prototype system in the field, its components were incorporated into watertight housings capable of being deployed to extreme depths. Umbilicals to each of were also constructed and interfaced to surface electronics for power and sampling.

The CV 5005-B camera fit neatly into a simple cylindrical housing shown above. The entire housing was just over 10 cm in length and less than 4 cm in diameter and constructed entirely of plastic to avoid corrosion. The main body of the housing was machined from a grey PVC rod upon a lathe. PVC is extremely strong and although not tested, was expected to provide a water-tight seal at depths of as much as one thousand feet. The body was comprised of four separate parts, two of which sealed the opposite ends of the housing with O-ring seals. This method of sealing the housing allowed the camera to be easily accessed through either end, a feature especially important since the camera was press fitted into place. It could therefore, only be removed by pushing it through the main sleeve of the housing. The end caps were locked into place by sliding a tie wrap through the channels created by the opposing grooves machined into the caps and the main housing sleeve.

A Seacon 5 pin wet mateable pigtail was bonded into the end cap of the housing using a two part, low viscosity, high strength black potting epoxy. Three of the five wires in the pigtail were then soldered to the three main wires of the bullet camera's cable. The red wire or the positive supply voltage of the camera was connected to the red counter part of the pigtail. The black wire or the Signal and Supply ground was likewise soldered to the black wire of the pigtail. The white wire or the video signal wire was also soldered to its pigtail counterpart. The mate of the underwater connector was soldered onto a 250 foot length of a neoprene jacketed, shielded, 2 conductor cable. The video and power wires were soldered to the center conductors while the signal and power ground was soldered to the braided shield of the cable. The splice was than wrapped and sealed using 3M self vulcanizing linerless splicing tape. A 9 pin plastic locking Amp connector was then attached to the surface end of the umbilical and mated with another cable with a power and RCA video plug to allow the camera to be plugged directly into a video port

P517410.PDF [Page: 30 of 47]

on a VCR or computer. Power was supplied with a standard 500 mA, 12V DC, AC power adaptor.

The window used for the housing was machined from acrylic rod upon a lathe and then hand polished to better than 5 μm for optimum clarity. The window was 1 cm in thickness with a circumferential o-ring seal against the main sleeve of the housing. The grey PVC end cap was used to lock this into place and prevent it from popping out under pressure from within the housing. An acrylic window was selected because of the relative ease by which it is machined and polished. It was also chosen however, since living marine creatures seem to prefer not to attach themselves to this plastic. Glass in contrast provides an ideal surface for silicaceous organisms such as diatom algae to attach themselves and grow. This effect accelerates optical attenuation by biological fouling and in moored applications can impede the operation of an optical instrument.

LED Projector Targets:

While it was essential to have a camera with both a high level of spatial resolution and sensitivity as the positional detector, it was also imperative that the target projectors have the optimal luminosity and beam properties. As mentioned previously, it was decided that LEDs were well suited for this application. These devices can be tailored to emit at a preferred wavelength by selecting the appropriate doping elements added to the silicon base chip. Their beams can also be easily tailored through the device's packaging since the emission from the actual semiconductor wafer is largely isotropic. Standard packages are typically in the form of a molded plastic unit with the actual semiconductor held in the center of parabolic reflector. The metal reflector functions both as an electrode and a light collector, and projects light through a lens formed into the clear plastic surrounding the electronic components. The dispersion of each particular device results from the balance of the focal lengths of the parabolic reflector and the plastic lens.LED packages come in a large number of different shapes and sizes and each have their own characteristic dispersion properties. The particular package selected for the projectors in this project was the most common and was designated as a T -1 ¾ package. This package

P517410.PDF [Page: 31 of 47]

was approximately 5 mm in diameter and 8 mm in length and the clear plastic of the body formed a single convex lens.

In order to develop a feeling for which beam properties would make the targets most detectedable, two different designs of target projectors were constructed. Each design used T -1 ¾ LEDs with emission peaks within the attenuation minimum of water. The first design used the natural beam pattern of a tight cluster of four LEDs. The second was an extrapolation of the first and utilized a 2.5 cm focal length condensing lens to compress the beam dispersion.

LED Projector Design I

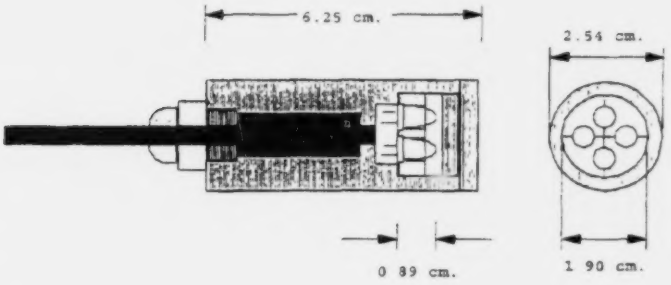

Figure 11: A cross-sectional side view and end on view of the first LED projector design.

The first of the target designs utilized a spectral spread from two different types of LEDs. One pair of LEDs were blue Sodium nitride LEDs with an emission peak near 470 nm. The other pair were of a new green-shifted design and had a peak emission near 490 nm. The intention of combining the two types of devices was that the two emission peaks would overlap to yield a broad emission peak centered near 480 nm the attenuation minimum of pure water. The blue pair (470 nm) however, were slightly more focused than the blue-green (490 nm) pair and as a result, appeared less intense. All however, had comparable emission intensities. These were greater than 3000 millicandles with a continuous forward current of 30 milliAmperes (mA). They were purchased from

P517410.PDF [Page: 32 of 47]

Chicago Miniature Lamps in Hackensack New Jersey and were of a standard T-1 ¾ package which provided them with a total beam dispersion of 30° or +/- 15° of center. The four devices were mounted in a machined plastic collar which held them as in Figure 11, within a cylindrical acrylic pressure housing. To one end of the housing an acrylic optical window was mounted with epoxy. To the other end, a water tight electrical penetrator was attached, also with epoxy. Each pair of the different LEDs were mounted on the opposing arms of a cross at 4.5 mm centers. Power was supplied via an epoxy filled box which held a printed circuit board with a board mounted pressure transducer (A Honeywell 26PCFFAGG), its amplifier, a 5 V regulator, and 10 V voltage regulator. Electrical current was supplied to each LED by the 5 V regulator and was held at 32 mA through 50 ohm series resistors. The epoxy filled box was attached to the surface through a 350 foot, 5 conductor PVC jacketed, ¼ inch cable and a 12 volt battery supply or a 12 volt DC power adapter. The pressure transducer was supplied 10 V from the one voltage regulator and its amplified output in DC volts was measured through an independent line in the cable using an analog to digital converter in a personal computer on the surface.

LED Projector Design II

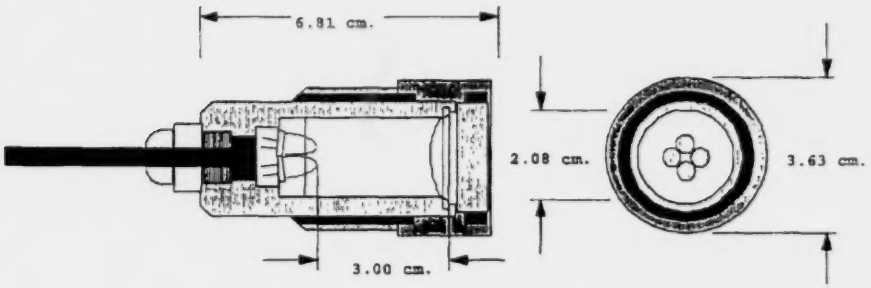

Figure 12: Cross-sectional side and end on views of the second LED projector design.

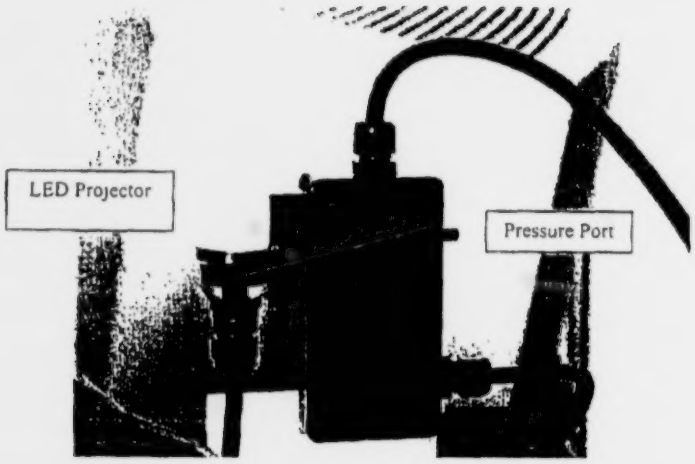

Figure 13: A picture of the projector mounted on the pressure sensor amplifier and voltage regulator module

The primary role of the second projector design was to optimize on the forward power density of the LED cluster's beam. This was done to minimize the light losses due to the inherent dispersion of the LEDs and increase the effective detection range of the projector. Like the first LED projector, the second design used a cluster of four high intensity LEDs. The second design however, had two fundamental design changes to optimize on its effective beam compression by a condensing lens. The first design change was the type of LEDs used. The blue-green LEDs used in the first design were not used since they appeared less focused and intense than the blue devices and the spectral advantages gained by their original addition were outweighed by the losses associated with their beam properties. The second design change to the LED cluster was that the four LEDs were physically packaged with smallest inter-unit distance possible and were secured into position to each other with epoxy. The devices were also canted inwards to the center of the cluster so that the smallest cross-sections of the LED lenses were aligned next to one another to reduce gaps even further.(see Figure 12). The cluster was then oriented and held in place with epoxy so that the axis of each LED passed through the center of a 2.5 cm single convex, glass condensing lens placed 3 cm from the tip of the

P517419 PDF [Page: 34 of 47]

cluster. Like the first design, the cluster was held within an acrylic pressure housing The power cable passed through the one end of the housing through a water tight compression fitting and black epoxy. On the other end, a 2.1 cm diameter, 2.5 cm focal length single convex lens was mounted with epoxy such that the flat surface of the lens face outwards. Over top of this lens, and the entire end of the acrylic cylinder a grey PVC cap with a 1 cm thick acrylic window was attached as in Figure 12 using black epoxy. The whole projector was then attached and connected to the same pressure sensing and regulating module used for the testing of first design. All of the original current constraints were therefore, applied to the second design with each LED receiving a forward continuous current of 32 mA.

Projector Beam Patterns:

The beam pattern of the first type of LED projector could only be resolved with the naked eye when it was physically held less than a metre from a reflecting surface such as a wall. The beam was very diffuse and as was mentioned previously, had a dispersion angle of approximately +/- 15°. The beam pattern of the second projector in contrast was visible at ranges as large as 10 metres. This projector generated a distinct clover leaf shaped pattern with each lobe provided by the beam of a blue LED. Both the width and height of the beam was 18 cm at a range of 1 metre and each lobe contributed 9 cm or half of these dimensions. This corresponded to a γ of 5° (See Equation 5) and each LED possessed a dispersion angle of 2.5° about its center. The light flux in the beam of the second projector therefore, was more than 9 times greater than that of the first since

$$\mathbf{E \propto 1/K}$$

$$\text{and,} \quad \mathbf{E_1 / E_2 = K(5) / K(15) = 9.29}$$

where E_1 and E_2 represent the beam flux of the two respective projectors.

PS17410.PDF [Page: 35 of 47]

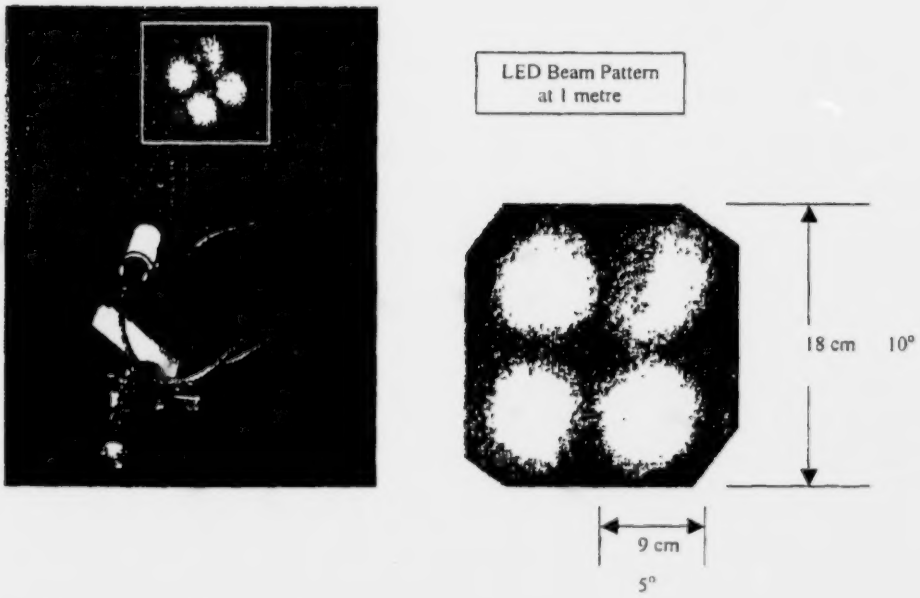

Figure 13: Images of the beam pattern of the second LED projector design.

Field Testing the Prototype System:

Field tests of the effective range of the prototype system were conducted both in freshwater and seawater. The freshwater experiments took place in a frozen lake called Hatchett Lake just outside of Halifax, Nova Scotia, Canada. For this experiment, both designs of target were range limit tested at night through holes cut in the ice. The camera was mounted horizontally and held approximately 0.3 metres below the bottom of the ice surface. It was aligned to view the target which was also mounted horizontally at a fixed range away. To obtain the range limit for each target design, the range was varied by moving the target through a series of different holes cut through the ice. The holes were set at 3.2, 6.5, 9.7, 19.4, 38.7, and 58 metres. Each time the image of the target was monitored with a television and an estimate of the maximum range was set at the point at which the image disappeared from the screen.

Two separate expeditions were undertaken within Bedford Basin in Halifax, Nova Scotia, Canada, to test the prototype system in seawater. The first took place after dark on December 21, 2000 and, the second on January 17, 2001. The tests were conducted at the deepest location of the basin where depths of as much as 240 feet or 77 metres were attainable. Deployments of the system were made from a 43 foot dive tending vessel called the MV Dive Com III from Connors Diving Services in Halifax. During deployments the vessel simply held position by maneuvering with its engine and monitoring its differential GPS. Vertical temperature profiles were collected prior to each deployment to identify the depth of the thermocline and the starting depth of potentially clear water for testing. The system's camera was then attached to the instrument package of the temperature profiler and deployed at or below the thermocline with its depth being provided by the unit's pressure sensor. In all instances, the camera was mounted looking downwards from the base of the instrument package and had a clear view of the water column beneath it.

During the first expedition, a single blue LED was mounted in a water tight housing at the end of a 2 metre post extending straight out from the base of the temperature profiler instrument package. The package was lowered to the base of the thermocline and the images of the camera recorded, to reference the center of the image grid and to qualitatively examine the scattering properties of the water at that time. While the camera and reference LED were still at depth, the LED target was lowered alongside, on a separate cable so that its image appeared at depths just greater than that recorded for the camera (See Figure 14). The target was lowered until it was no longer visible on a television screen and its range D was calculated from the temperature profiler and target pressure transducers using a personal computer and interface card on deck. In order to avoid contamination of the AGC by the reference LED, the procedure was repeated without the post and LED present. During all deployments the video images were recorded upon a video tape with a VCR.

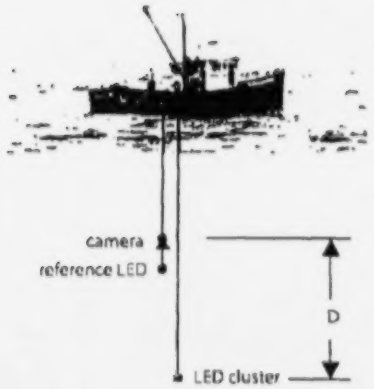

Figure 14: A diagrammatic representation of the prototype system during the first expedition. In this image the reference is mounted with the camera to provide a center for the image's axis

The second expedition used much the same procedures as the first to quantify the maximum range of the second type of LED target projector. The only difference was that the measurements were repeated for two different depth ranges. The first range spanned depths between 32 and 55 metres while the second began at 44 metres and extended down to approximately 70 metres. As in the first expedition, the maximum value of D was recorded as the range limit when the target could no longer be seen on the television screen.

Results and Discussion

Range Limit Testing in Air:

The results of the analysis of the range limit of the prototype system with the neutral density filters suggested that detection ranges of as much as 65 metres were

P517410.PDF [Page: 38 of 47]

possible underwater but only with the second design of LED projector. It appeared that the dispersion of the first design limited detection to ranges closer to 40 metres.

During the tests the size of the target and the width of its associated peak, decreased with increased range until only a single pixel was illuminated. The amplitude of the image's peak remained constant until the limits of the AGC were reached and then rapidly decreased until the image was no longer resolvable in the background.

Range Limit Testing in Water:

The results of the range limit tests conducted in Bedford Basin suggested that the maximum viewing envelope was substantially smaller than that predicted by the tests in air. During these tests, the first design of LED projector could be detected up to 18 metres away from the camera. The second design in contrast could be detected up to 23 metres from the camera. These values were less than half of those from the tests with neutral density filters. The difference was likely the result of the large amounts of suspended particles visible in the images observed on both expeditions. The fact that no clear thermocline could be resolved on both occasions suggested that the water column had been mixed by several consecutive wind storms, to depths greater than those in the basin. This meant that even though the experiment was conducted in the winter when phytoplankton concentrations are normally at their lowest, they may have also been present to absorb the target's light before reaching the camera. In any instance, the tests clearly showed that attenuation by materials in the water can under certain circumstances severely impede the detection range of the system. This was further exemplified in the results of the range limit testing in the freshwater lake under the ice. Here the effects of what were believed to be dissolved organic substances called humic acids, limited the range of the system to less than 7 metres. Even the second design of target projector could not penetrate more than 4 metres during the one particular day. Such conditions however, are only expected to occur in near shore waters where run off from lakes and

P517410.PDF [Page 39 of 47]

rivers introduce a variety of potential attenuators into the upper water layers (Wetzel 1975).

How the Camera Viewed the Targets:

As was mentioned previously, the role of the projector was two fold: (i) to maximize on the projection of the LED light towards the camera, and (ii) to ensure that the beam spot image provided a clean well resolved voltage peak in the raw video signal. In the first projector design, the packaging of each of the individual LEDs dictated how the light was emitted from the pressure housing underwater. Light emitted was projected evenly over four overlapping 30° cones. It therefore, appeared diffuse and when viewed underwater, as if it were from a point source emitter. The result was a clean Gaussian type voltage peak in the video signal. This type of image is preferred since it allows the intensity peak to be directly associated with the center of the projector. The series of images collected in Figure 15 show the uniformity of the light as viewed by the camera. What is also of particular interest in this particular series of images is the similarity between the view of the single reference LED and the view of the projector at various ranges below. This results from two primary effects associated with the resolution of the camera and the scattering properties of the water. Since the angular resolution of the camera is near 0.2° the camera can only resolve individual LEDs in the cluster at ranges which are less than 3 metres. The other factor, is the smearing of the projectors image by scatterers in the water.

Figure 16 is a diagrammatic representation of how a vertical array of the targets might look on an oscilloscope sweep of the video frame or line signal. The diagram illustrates how the shape of the target's image can be expected to change with range. In the figure, distant targets B-J have well defined peaks. Target A however, was within what can be called the near field of the system where intensities saturated the CCD elements. Here the top of the image's peak became flattened and too wide to provide a good position estimate.

P517410.PDF [Page: 40 of 47]

Figure 15: An image of the reference LED and a series of the target projector Design I as it was being lowered below the camera in Bedford Basin

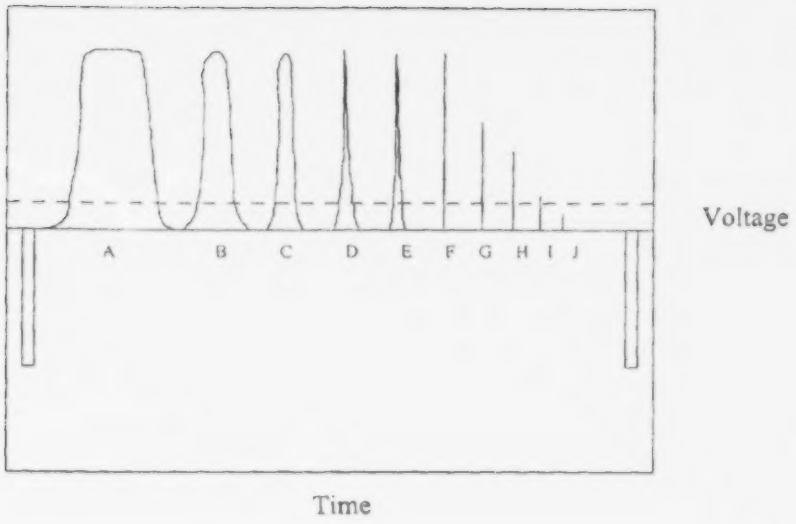

Figure 16: A diagrammatical representation of a series of different target images generated by targets at increasing ranges (from left to right). The diagram presents how the AGC of the CV 5005-B ajusts the peak shape during normalization It is based on the oscilloscope scans of the video images presented in Figure 15. The dashed line represents the minimum voltage threshold of the television. The negative going pulses are the line or frame sync. pulses.

The effects of the beam shape and saturation were particularly noticeable in the images of the second type of target projector. With this design, intensities were so great that light from scatterers in the beam distorted the shape of the image. Figure 17 shows these effects quite well. Here the actual lobes of the beams can be resolved in scattering from the particles suspended in the beam. These lobes however, are only expected to add to a target peak already broadened by saturation of the CCD matrix by the center of the target beam.

The limitations imposed by the use of intense target projectors could be reduced with one of two modifications. The easiest requires the scaling of LED intensities based on their position in an array. The approach however, requires some pre-determined knowledge of the attenuation properties of the water column. The alternative requires the camera's AGC to be modified or the use of an AGC amplifier with both a wider

0617410.PDF [Page: 42 of 47]

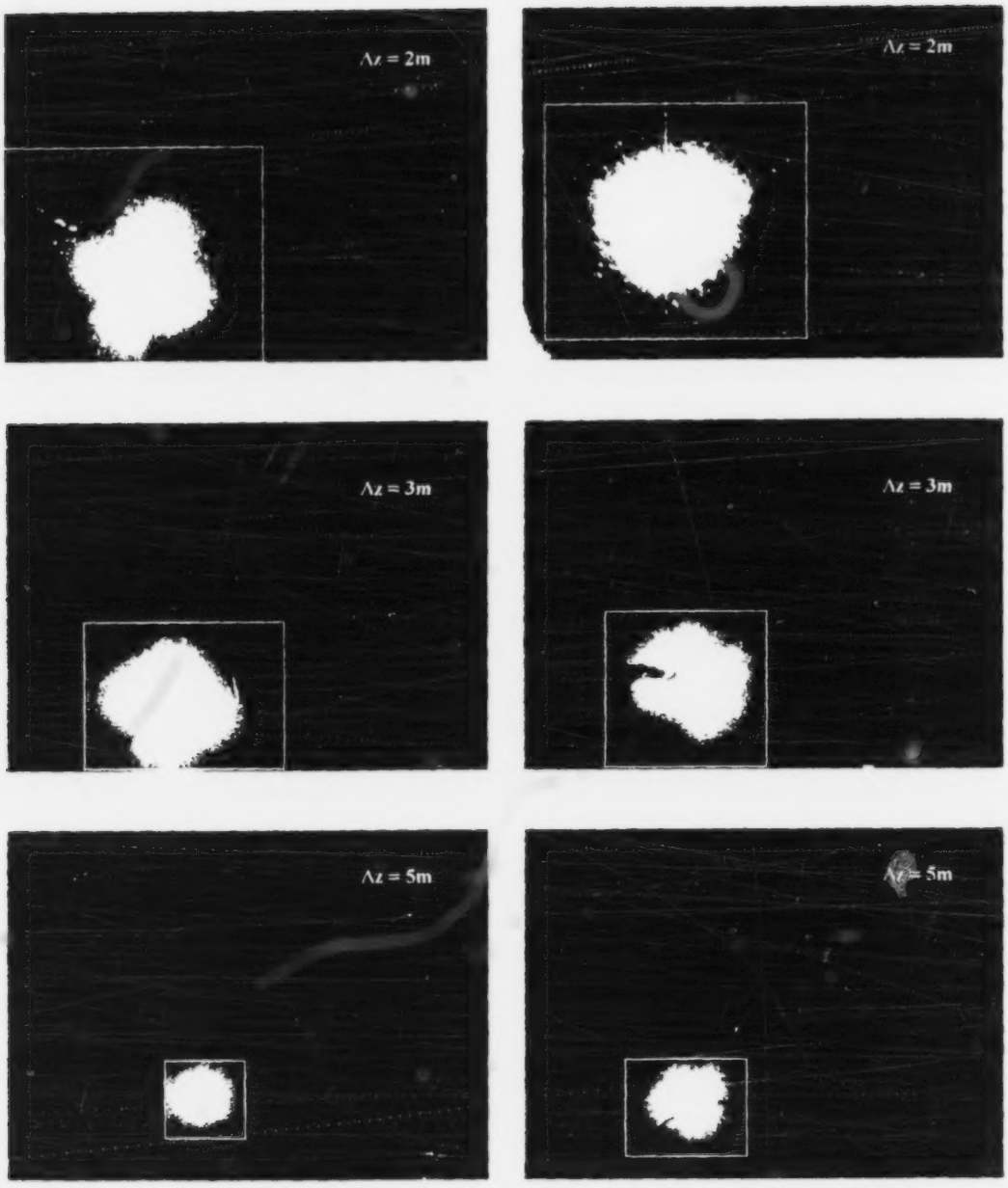

Figure 17 (a): The following are images of the LED projector Design II as seen by a black and white video camera. The images were taken with the camera being held at a depth of 30 metres and the projector at the stated range vertically below the camera. Δz is the depth separation between the camera and the projector.

P512410.PDF [Page: 43 of 47]

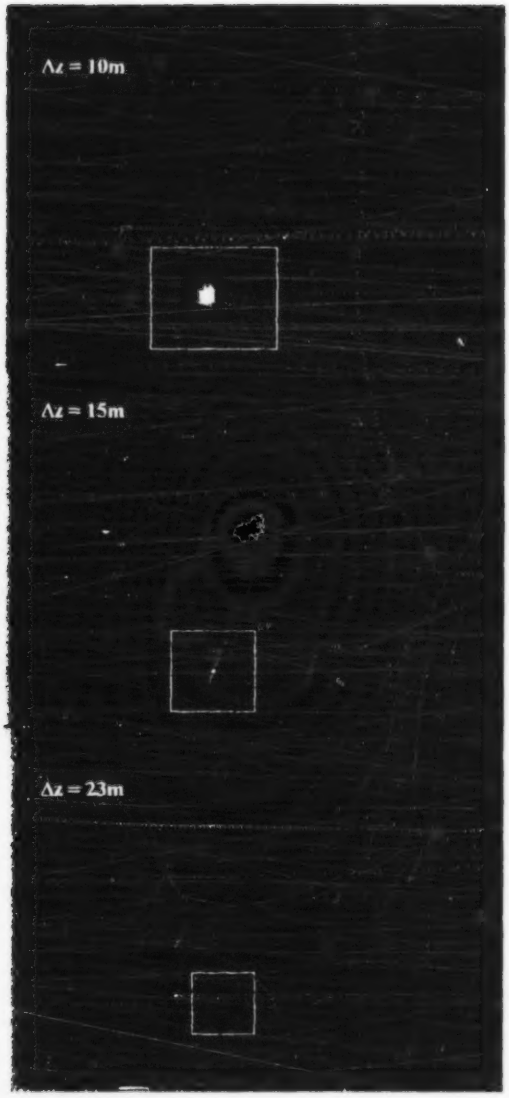

Figure 17 (b) LED projector Design II images at depths where the image was of an intensity near the lower limits of the camera's AGC amplifier In the lowest image the target is just barely visible and could only be seen by watching its motion on the television screen

P517410.PDF [Page: 44 of 47]

dynamic range and more steps within this range. While both techniques should work, the final design will likely incorporate a balance of the two to optimize on the systems capabilities.

Conclusions

In conclusion then, the results of the tests with the prototype positioning system suggested that the conceptual system could be a valuable tool for correcting mooring shape distortions. They also clearly indicated that the conceptual system could be constructed with commercially available technologies at reasonable costs. The only limitations envisioned were the result of limitations in the commercial camera system and the luminosity of the particular LEDs used in the experiments. Both limitations are still curable with the assistance of the manufacturer's of the particular devices.

References

Morel, A., Optical properties of Pure Water and Pure Seawater, in Optical Aspects of Oceanography, Edited by Jerlov N.G. and E. Steelmann Nielsen, pp 1-23, Academic Press, London and New York, 1974.

Tyler, J.E., and R.C. Smith, Measurements of spectral radiance underwater, Gordon and Breach Science Publishers, N.Y., 1970.

TRW Optoelectronics Data Book, pp 75, TRW Optoelectronics Division, Carrollton, Texas,
1985.

Wetzel, Robert. G. Limnology, pp 55-56, W.B. Saunders Company, Philadelphia, U S , 1975.

UNCLASSIFIED
SECURITY CLASSIFICATION OF FORM
(highest classification of Title, Abstract, Keywords)

DOCUMENT CONTROL DATA

(Security classification of title, body of abstract and indexing annotation must be entered when the overall document is classified)

1 ORIGINATOR (the name and address of the organization preparing the document Organizations for whom the document was prepared, e g Establishment sponsoring a contractor's report, or tasking agency, are entered in section 8)

Marentec, 6 Jamieson St., Suite 23, Dartmouth, NS

2. SECURITY CLASSIFICATION (overall security classification of the document including special warning terms if applicable)

UNCLASSIFIED

3 TITLE (the complete document title as indicated on the title page Its classification should be indicated by the appropriate abbreviation (S,C,R or U) in parentheses after the title)

A feasibility study of an optical positioning system to correct for dynamic hydrophone array shape variations

4 AUTHORS (Last name, first name, middle initial If military, show rank, e g Doe, Maj John E)

Richard D. Dittman

5 DATE OF PUBLICATION (month and year of publication of document)	6a NO OF PAGES (total containing information Include Annexes, Appendices, etc)	6b NO OF REFS (total cited in document)
March 2001	34 (approx.)	4

7 DESCRIPTIVE NOTES (the category of the document, e g technical report, technical note or memorandum If appropriate, enter the type of report, e g interim, progress, summary, annual or final Give the inclusive dates when a specific reporting period is covered)

CONTRACTOR REPORT

8 SPONSORING ACTIVITY (the name of the department project office or laboratory sponsoring the research and development Include address)

Defence Research Establishment Atlantic
PO Box 1012, Dartmouth, NS, Canada B2Y 3Z7

9a PROJECT OR GRANT NO (if appropriate, the applicable research and development project or grant number under which the document was written Please specify whether project or grant)	9b. CONTRACT NO (if appropriate, the applicable number under which the document was written)
5aa11	W7707-008102/001/HAL

10a ORIGINATOR'S DOCUMENT NUMBER (the official document number by which the document is identified by the originating activity This number must be unique to this document)	10b OTHER DOCUMENT NOs (Any other numbers which may be assigned this document either by the originator or by the sponsor)
DREA CR 2001-021	

11 DOCUMENT AVAILABILITY (any limitations on further dissemination of the document, other than those imposed by security classification)

(X) Unlimited distribution
( ) Defence departments and defence contractors; further distribution only as approved
( ) Defence departments and Canadian defence contractors; further distribution only as approved
( ) Government departments and agencies; further distribution only as approved
( ) Defence departments; further distribution only as approved
( ) Other (please specify):

12 DOCUMENT ANNOUNCEMENT (any limitation to the bibliographic announcement of this document This will normally correspond to the Document Availability (11) However, where further distribution (beyond the audience specified in (11) is possible, a wider announcement audience may be selected)

UNCLASSIFIED
SECURITY CLASSIFICATION OF FORM
UNCLASSIFIED

P517410.PDF [Page: 46 of 47]

13. ABSTRACT (a brief and factual summary of the document. It may also appear elsewhere in the body of the document itself. It is highly desirable that the abstract of classified documents be unclassified. Each paragraph of the abstract shall begin with an indication of the security classification of the information in the paragraph (unless the document itself is unclassified) represented as (S), (C), (R), or (U). It is not necessary to include here abstracts in both official languages unless the text is bilingual)

The following report describes an analysis of a conceptual optical positioning system for measuring the shape of a hydrophone array underwater. The analysis involved the design and construction of a prototype test system comprised of commercially available electronic components. The conceptual system determined the shape of an underwater mooring by positioning tracking targets mounted at fixed points along the mooring. The prototype used a small sensitive black and white camera as the positional detector and high intensity light emitting diodes as tracking targets. The system was examined for its potential range capabilities and spatial resolution underwater. Tests were specifically conducted on the range limits of the system in air, freshwater, and seawater. The results suggested that the spatial resolution of the system was better than 26 cm with target ranges as great as 65 metres. They also indicated, however, that water born attenuators could dramatically reduce the systems operational range limit. Field tests within near-shore waters of Nova Scotia, for example, found range limits closer to 20 metres.

14. KEYWORDS, DESCRIPTORS or IDENTIFIERS (technically meaningful terms or short phrases that characterize a document and could be helpful in cataloguing the document. They should be selected so that no security classification is required. Identifiers, such as equipment model designation, trade name, military project code name, geographic location may also be included. If possible keywords should be selected from a published thesaurus, e.g. Thesaurus of Engineering and Scientific Terms (TEST) and that thesaurus-identified. If it not possible to select indexing terms which are Unclassified, the classification of each should be indicated as with the title).

LED
underwater positioning system